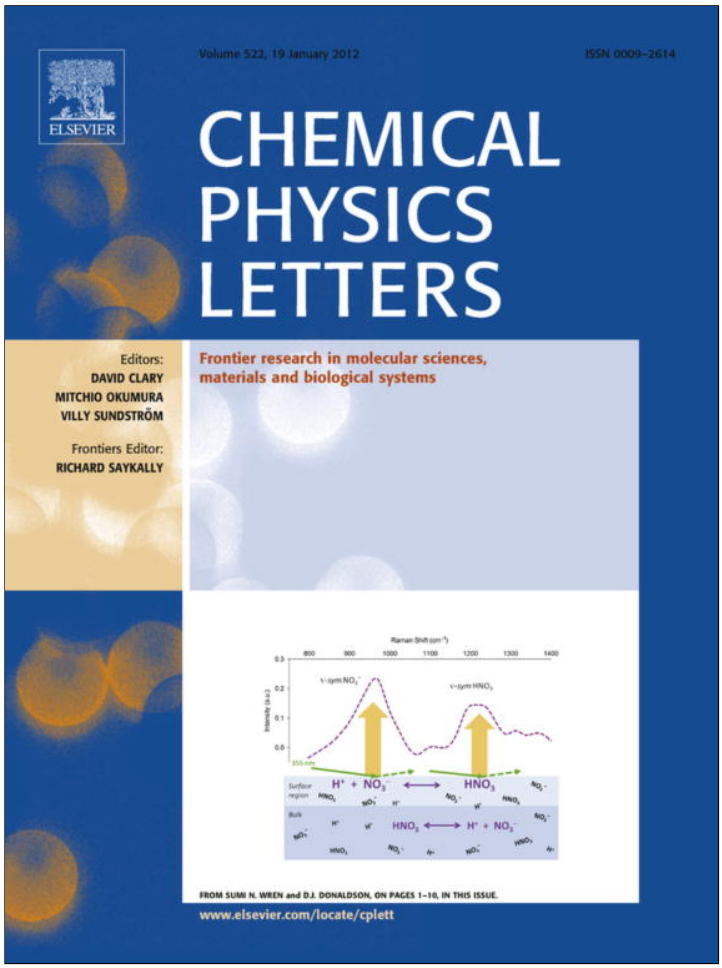

Chemical Physics Letters 522 (2012) 23–27

Contents lists available at SciVerse ScienceDirect

Chemical Physics Letters

journal homepage: www.elsevier.com/locate/cplett

Ionization of naphthalene via the Rydberg states using a femtosecond 775 nm pulse

Motoshi Goto *, Klavs Hansen

Department of Physics, University of Gothenburg, 41296 Gothenburg, Sweden

ARTICLE INFO

Article history:
Received 30 October 2011
In final form 5 December 2011
Available online 11 December 2011

ABSTRACT

Photoelectron spectroscopic studies on naphthalene excited with a femtosecond 775 nm laser pulse reveal two ionization paths via the Rydberg states: a resonance-enhanced, non-relaxed process and one that goes through internal conversion of an undetermined intermediate. Varying the pulse duration with several hundred femtosecond causes only small change in the spectra. Compared to the ionization mechanism of anthracene, the reduced molecular size changes the ionization behavior due to a slower internal conversion rate and the presence of atomic-like Freeman resonances.

1. Introduction

Laser intensity is one of the critical parameters determining the ionization mechanism of atoms and molecules. An important part is played by the ponderomotive energy, U_p, which is the energy that a free electron acquires in the rapidly oscillating laser field, and which is given by the equation: $U_P = e^2I/2c\epsilon m_e\omega^2$. Here, e is the charge of the electron, I the laser intensity, c the speed of light, ϵ the vacuum permittivity, m_e the mass of the electron and ω the frequency of the laser field. Accordingly, in a laser field, the ionization energy of a target, IE, rises by the value of U_p, proportional to the intensity.

For intensities below the field ionization regime, which is the regime explored in the present work, the ionization of atoms takes place through vertical non-relaxed multiphoton processes. The resulting photoelectron spectra (PES) show above threshold ionization (ATI) [1] made possible by resonances due to a U_p shift of Rydberg states, called Freeman resonance [2]. For molecules, two other ionization channels open in addition to the vertical process. One is ionization from Rydberg states created via internal conversion (IC), that is, electronic relaxation from an intermediate state prepares electrons in these states, from which a photoabsorption process ionizes the molecule [3]. In the other channel, the energy of the absorbed photons is stored in incoherent electronic excitations and the ionization occurs (quasi-) thermally before the energy is coupled to the molecular vibrations. This channel has been observed for several large molecules and clusters [4–6].

To understand the transition of the ionization mechanisms from the atomic-like ATI behavior to the large molecular quasi-thermal ionization, we have studied how the ionization mechanisms depend on molecular size, using polyaromatic hydrocarbons as a model system [7,8]. A relatively large molecule, such as coronene ($C_{24}H_{12}$), only ionizes by the quasi-thermal process, while on the other hand the smaller molecule anthracene ($C_{14}H_{10}$) clearly switches channels depending on the characteristic of the laser pulse. In particular the duration influences the ratio between the vertical and the IC-assisted processes. Also, for higher intensities the thermal process becomes dominant. From these studies it appears that the relaxation processes are crucial ingredients in the molecular ionization process. Thus, the ionization behavior of molecules smaller than anthracene is an interesting issue and may answer questions such as whether the ionization mechanism for these is similar to that of anthracene, or if different, clarify the role of the relaxation process.

Here we report measurements of PES of naphthalene ($C_{10}H_8$) and compare them with earlier result on anthracene. One may expect that the ionization behavior of naphthalene is closer to that of an atom (but by no means identical to) than similar quantities for anthracene. It will be shown in this work that there is indeed a significant difference between the ionization behavior of anthracene and naphthalene. The vertical ionization is very pronounced for naphthalene, and the IC-assisted ionization is observed as well, while the contribution of the thermal process is negligibly small. The relative yield of the first two paths did not change significantly with the pulse duration. We will explain these observations in terms of an IC rate which is smaller for naphthalene than for anthracene, and we will suggest that the resonance structure which plays an important role for ATI will also be important for IC mediated ionization. Consequently, the present report corroborates our previous conclusion that the IC is a determining factor for the branching into the different ionization channels.

2. Experiment

The experimental setup has been described elsewhere [5]. In brief, commercially available naphthalene (ACROS ORGANICS, 99+% purity) was used without any further purification, and put

* Corresponding author.
E-mail addresses: motoshi.goto@physics.gu.se (M. Goto), klavs.hansen@physics.gu.se (K. Hansen).

0009-2614/$ - see front matter © 2011 Elsevier B.V. All rights reserved.
doi:10.1016/j.cplett.2011.12.006

in a sample holder to produce an effusive molecular beam. The material sublimes very easily and the pressure inside the vacuum chamber was on the order of 10^{-6} to 10^{-5} mbar. The molecular beam was crossed with a focused laser pulse whose wavelength was 775 nm (1.6 eV) and the generated electrons were monitored with the imaging apparatus described in [5].

The inversion of the raw data images was performed with the procedure reported in [9] and a calibration with the ATI peaks provided the energy scale for the PES. An example of a raw image and the corresponding inverted image, as well as the angle-integrated PES, are shown in Figure 1. The electron signal below 0.1 eV is due to ionization of pump oil, which appears especially when the intensity is high and the pulse has a long duration. The data in this region are ignored throughout the present study.

The laser intensity was determined by measuring the Freeman resonance of xenon gas under the same condition as the measurements on naphthalene. The shortest duration of our laser is 150 fs, and the durations of the stretched pulses were evaluated also from the xenon PES, assuming that the size of the focal point is independent of the duration.

The value of *IE* of naphthalene is 8.15 eV [10]. This means that at least six photons are necessary to ionize and the kinetic energy of the emitted electrons is 1.45 eV for this number of electrons, ignoring ATI and U_p shift.

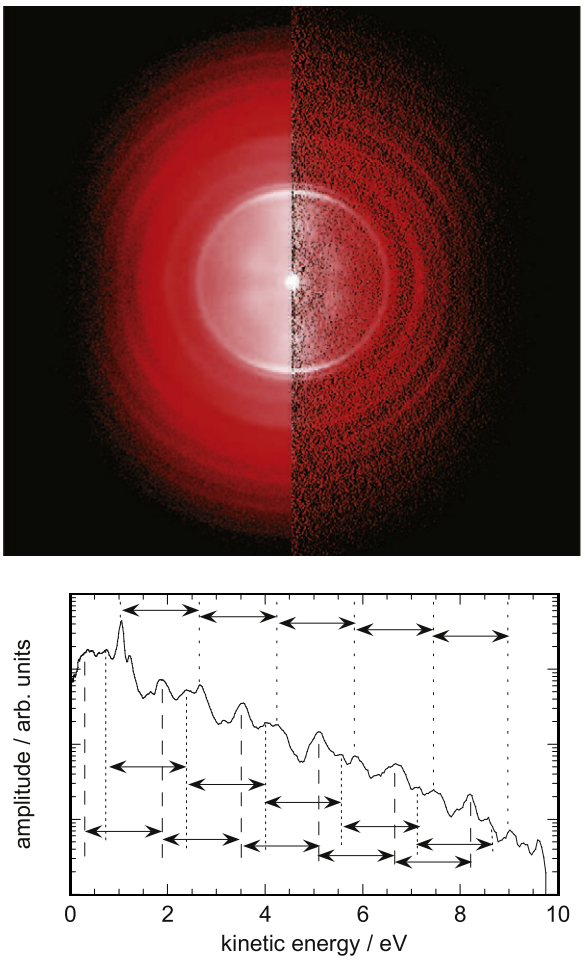

Figure 1. An example of the experimental results. Top: the raw image (left half) and the corresponding inverted image (right half) for the laser intensity of 1.3×10^{13} Wcm^{-2} and the duration of 150 fs. The color scale is logarithmic and covers three orders of magnitude. The laser polarization is in the vertical direction. Bottom: semi-log plot of the angle-integrated PES of the inverted image. In this experimental setup, the highest observable electron energy is about 9.8 eV, seen as the cut-off of this PES. The length of the arrows correspond to one photon energy (1.6 eV).

Compared to an earlier work on PES of naphthalene [11], we have used lower laser intensity (less than 40%) and added an imaging equipment for the detection of electrons. This has allowed us to focus on PES in the low energy region to study the relation between U_P and the spectral feature in detailed.

3. Results and discussion

In this section, we analyze how the PES depend on the intensity and the duration and discuss the similarities and differences in the ionization behavior of naphthalene and anthracene.

3.1. Analysis of the low energy region below IE

The intensity dependence of the PES below $6h\nu - IE$ and in particular the effect of U_p on the spectrum in this region provide important clues as to the ionization mechanism. Zoomed PES are given in Figure 2, and indicate that the spectral structure depends strongly on the intensity.

For the intensity of 0.51×10^{13} Wcm^{-2} (the bottom PES), admittedly with low statistics, the peaks centered at 1.32, 1.22, 1.03 and 0.60 eV (denoted as P_1, P_2, P_3 and P_4, respectively) appear below the *IE*, and P_3 and P_4 are also below the energy of $IE - U_p$. Because U_p is low, the vertical process cannot produce such low energy electrons, and they must therefore be assigned to IC-assisted processes. This demonstrates the existence of one or more intermediate states.

In Figure 2, one clearly sees that the role of the most intense peak shifts towards lower energy peaks as the intensity increases. From the lowest to the second lowest intensities, P_2 and P_3 grow and P_2 is higher than P_3, and simultaneously the others become smaller. As the intensity increases, P_3 becomes higher than P_2, and at the intensity of 1.3×10^{13} Wcm^{-2}, P_3 dominates the spectrum. For the two highest intensities, P_3 is suppressed, and instead a broad peak centered at 0.75 eV (denoted as P_5) appears.

This behavior can be explained in terms of Freeman resonances, which have been observed not only for atoms but also for small molecules [14,15]. That is, when the sum of U_p and the energy difference between ground and a given Rydberg state is a multiple of a photon energy, in this case $5h\nu$, the ionization probability increases dramatically. Provided that the energy difference between the *IE* and each Rydberg level is independent of the intensity, both the vertical resonant and the IC-assisted processes occurring from a given Rydberg state produce a fluence-independent electron energy. Energy considerations are therefore not enough to assign a peak to either mechanism. Independent evidence to either assignment is the presence or not of a peak above the energy $6h\nu - IE - U_p$, where a presence indicates that the peak appears via IC, and the absence of a peak suggests that it is generated in a resonant process.

As mentioned, the relative amplitude between P_2 and P_3 is reversed when the intensity is varied from 0.64 to 0.90×10^{13} Wcm^{-2}. These intensities correspond to U_p values of 0.34 and 0.50 eV, respectively. Thus, only for the highest of these two intensities is the U_p larger than the difference in energy (0.42 eV) between P_3 and the *IE*. Based on this, the observation made about their peak amplitudes indicates that while the IC-assisted process gives P_3 even for the lower intensity, the resonant process from this level is active only for the highest of the two intensities. Also, since the energy difference of P_5 from the *IE* is 0.70 eV, the three highest intensities (U_P = 1.2, 0.95 and 0.73 eV) are expected to give rise to resonant ionization from this state, but not for the lowest three intensities. At the third highest intensity with $U_p = 0.73$ eV, P_5 is not clearly displayed in the spectrum,

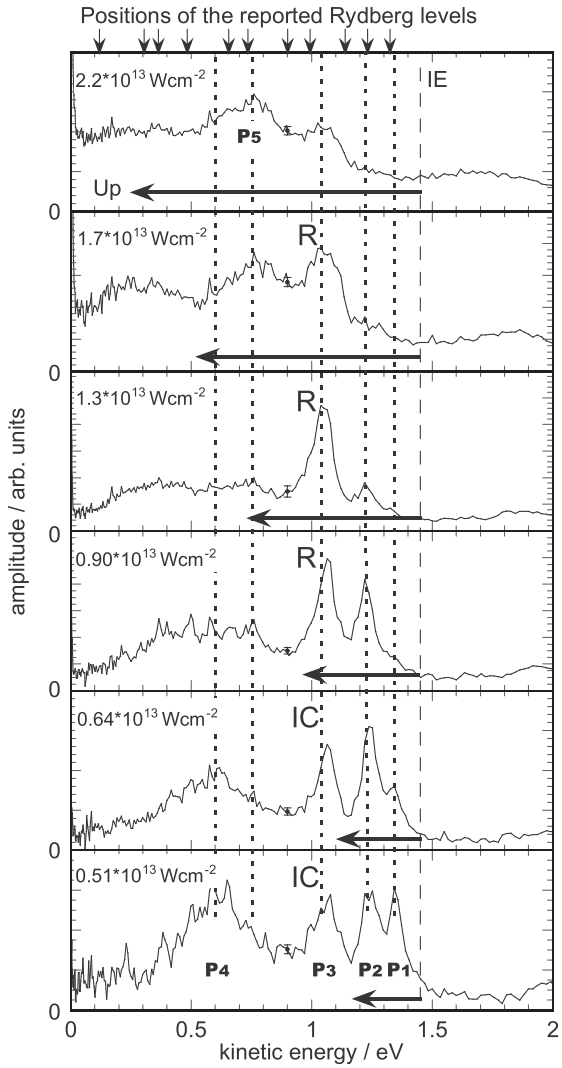

Figure 2. Angle-integrated PES below 2 eV for six different intensities, given in the upper left corner of each spectrum. The pulse duration is 150 fs. Error bars at the kinetic energy of 0.90 eV show the standard deviation of the signals in the region from 0.85 to 0.95 eV. The energy of '*IE*' electrons shown in this figure is $6h\nu - IE$, ignoring the U_p shift. Corresponding U_p values are shown as the length of arrows from the energy of *IE* drawn in the bottom of each spectrum. The vertical dotted lines indicate the peak positions found in this work. P_{1-5} designate the different peaks described in the text. 'IC' and 'R' indicate the IC-assisted and the resonance enhanced ionizations, respectively, for the ionization path of P_3 at different intensities (see text). The PES for 1.3×10^{13} Wcm^{-2} is from the spectra shown in Figure 1. The arrows on top are the observed peak positions in [12,13]

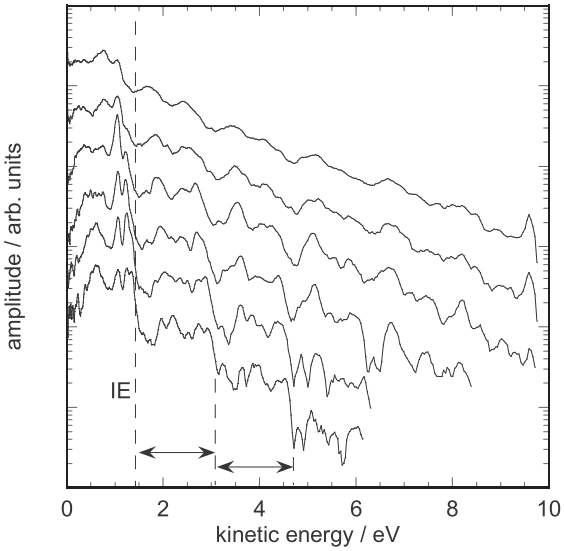

Figure 3. Semi-log plot of the PES shown in Figure 2 but up to 10 eV. The intensities are 2.2, 1,7, 1.3, 0.90, 0.64 and 0.51×10^{13} Wcm^{-2} from top to bottom. The length of each horizontal arrow corresponds to one photon energy (1.6 eV) and the vertical dotted lines illustrate the energy of *IE*, $IE + h\nu$ and $IE + 2h\nu$. The PES for the intensity of 1.3×10^{13} Wcm^{-2} is the same curve as that shown in the bottom of Figure 1. These PES are shifted for display purposes.

presumably because the intensity is close to the threshold. For the two highest intensities, however, P_5 is readily apparent. For this reason, we identify the observed tendency as the result of resonant non-relaxed ionization.

Earlier works have reported the detection of Rydberg states of naphthalene populated through the IC mechanism for two different wavelengths under conditions where U_p is negligibly small, and confirmed that the spectral features are basically independent of the wavelengths [12,13]. Comparing the present results with these spectra (the arrows on top of Figure 2 illustrate the positions of the Rydberg energy levels in [12,13]) we see that our main peaks except P_4 coincide with the reported levels within 0.03 eV, supporting the validity of the conclusions made above.

Several features are new in our spectra, however. In particular, the peak P_4 has not been observed previously, and in the top spectrum in Figure 2 (2.2×10^{13} Wcm^{-2}), no peaks are detected in the region below 0.6 eV despite a sufficiently high U_p value to allow such peaks. We offer here possible explanations for these two observations. As for the first, we suggest that the initial state of the P_4 peak is populated only through IC from the initial state of the P_1 peak. This is based on the facts that the amplitude of these peaks decreases, while on the other hand their relative yield stays almost constant as the laser intensity is changed from the lowest to the second lowest values, and secondly that they disappear for intensities at or higher than 0.90×10^{13} Wcm^{-2}. Because P_1 was observed to be a weak peak in the earlier reports [12,13], where the U_p was very low, we conclude that the resonance process is responsible for the significant enhancement of the strength of P_1 seen here, as well as the accompanying enhancement of P_4.

The observation that peaks are absent from the low energy region (below 0.6 eV) can be explained as a consequence of the fact that the IC-assisted ionization dominates over the resonance process in this region. For 0.90×10^{13} Wcm^{-2} we see a structureless signal in this region, where only an IC-assisted process is active. The relative intensity of this signal increases with increasing laser intensity. At higher laser intensities the IC-assisted channel is therefore populated more efficiently than the resonant ionization, and consequently no noticeable peaks are detected.

3.2. Analysis of the energy region above IE

Because the thermal emission process gives a smooth PES that is well described as an exponential function [16], it is relevant to analyze the PES over a wider energy range. Inspection of Figure 3, which is the same PES as shown in Figure 2 but for kinetic energy up to 10 eV, shows ATI structures in all PES. In a more detailed analysis of the PES in the bottom of the figure, the comparison of signal amplitudes among the energy regions from 0 to *IE*, from *IE* to $IE + h\nu$, and from $IE + h\nu$ to $IE + 2h\nu$ indicates that the amplitude decreases dramatically for higher energy regions but is otherwise quasiperiodic in the photon energy. This is a sign that the spectral features are governed by the ATI process for the energy higher than *IE*, especially the IC-assisted process due to the low U_p value (see the PES in the bottom of Figure 2), not by the thermal process.

This structure in the spectra is observable for the higher intensities but as the intensity increases, the structure in the PES is washed out and higher intensity spectra show smoother energy distributions. Concentrating on the peaks centered at 2.0 and 2.8 eV and their ATI series for the intensity of 0.90×10^{13} Wcm^{-2}, we see that these peaks get increasingly broader at higher intensities, and that eventually the peak broadening produces a smooth, exponentially decreasing spectral shape at high intensities. Although a smooth high energy part of the spectrum is symptomatic for a quasi-thermal emission process, it is not unique to this mechanism and in the case of naphthalene we must assign the smooth distribution to reasons other than hot electron emission.

The ATI structures seen in Figure 3 exhibit an interesting behavior related to the relative strength of vertical ATI processes and IC mediated ionization. For example, at the intensity of 1.3×10^{13} Wcm^{-2}, the comparison between the two series starting with 0.3 and 1.0 eV, which correspond to the IC-assisted and the vertical ionizations, respectively, provides evidence that the former yields stronger ATI signals (defined as $6 + n$ ($n \geqslant 1$) photon processes) than the latter, and that this tendency increases with the order of the process (see also Figure 1 for an easier comparison). This is likely to originate in the fact that the IC-assisted ionization is a two-step photoabsorption process, albeit occurring in a single pulse: the first step prepares a Rydberg state through the IC and the second causes the ionization from that state. As a consequence, the process is approximately a $1 + n$ (to ionize) or a 5 (to populate the Rydberg state) photon process, whereas the vertical process requires at least six photons, leading to the higher probability of ATI for the IC-assisted process.

3.3. Duration dependence

As discussed above, the analysis of the ATI structure suggests that the IC-assisted channel is described in terms of a two-step photo-ionization process. Assuming that the second step (the ionization) occurs at the peak intensity, the dependence of PES on the pulse duration when the peak intensity is kept constant provides a clue about the lifetimes of intermediate and Rydberg states.

PES for three different pulse durations are shown in the top of Figure 4 recorded at the intensity 1.1×10^{13} Wcm^{-2}, where P_3 is the strongest peak. They differ by a small duration dependence of the ratio of P_3 and the featureless signal in the region between 0.1 and 0.8 eV, to which only the IC-assisted ionization contributes due to the low U_p value. The strength of the P_3 peak becomes relatively less pronounced for longer pulse duration. Describing these two spectral regions in any detail requires accounting for the initial excitation to the resonance, the direct ionization from this state, the IC rate for crossing into the Rydberg state, the decay rate of the Rydberg state and the ionization rate of the Rydberg state. This scheme is illustrated in the bottom of Figure 4. A complete description is not possible with the present data, but a few conclusions can be drawn. First, the resonant states are populated before the intensity is peaking, whereas the ionization from the IC states occur at peak intensity. This means that the lifetime of the resonant states (τ_1 in Figure 4) must be less than or equal to a fraction of the shortest pulse duration. The Rydberg states, on the other hand, must have a lifetime (τ_2) that is longer than or at least similar to the same fraction of the duration of the longest pulse, because otherwise the decay would prevent the ionization of these species.

3.4. Comparison of the ionization behavior of naphthalene and anthracene

We now discuss the difference between the ionization mechanisms of naphthalene and anthracene. As seen Figure 3, the PES has clearly discernible ATI peaks, even for the high intensity of

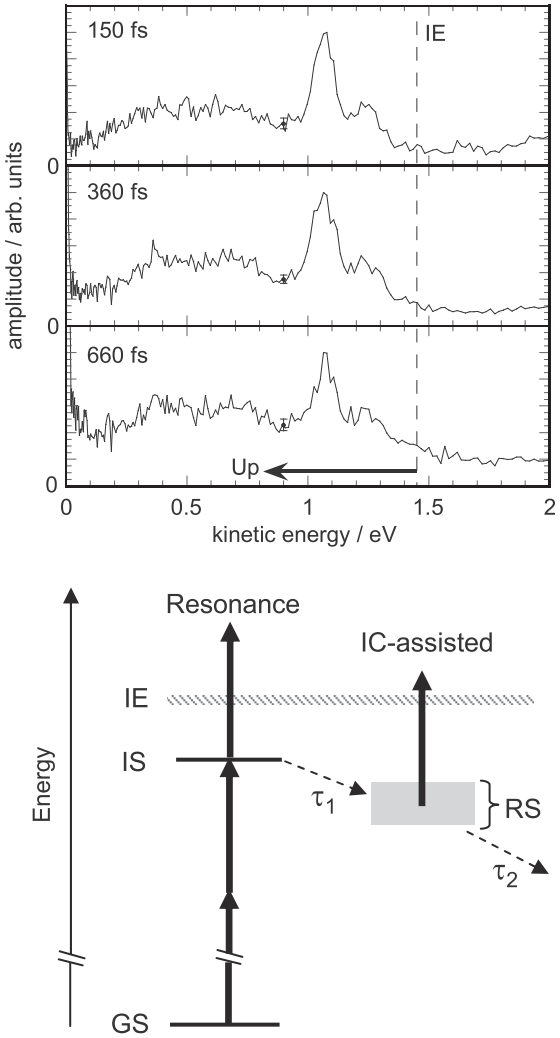

Figure 4. Top: angle-integrated PES below 2 eV measured as the spectra in Figure 2, but for three different durations, given in the upper left corner of each spectrum. The intensity is 1.1×10^{13} Wcm^{-2} for all. The spectra are normalized to the amplitude of the strongest peaks, which corresponds to P_3 in Figure 2. For the information on the error bars, see the caption of Figure 2. Bottom: schematic view of the energy level diagram which illustrates the ionization scheme discussed in the text. Vertical arrows indicate $h\nu$, GS is the ground state, IS is an intermediate state, RS denotes Rydberg states, τ_1 is the lifetime of the IS, namely 1/(IC rate), and τ_2 the lifetime of the RS.

2.2×10^{13} Wcm^{-2}. It is of interest to compare it with the PES for anthracene that have similar logarithmic slopes on the high energy tail, as for example the curve for 1.1×10^{13} Wcm^{-2} in Fig. 10 of reference [7]. Apart from the fact that the PES for anthracene contains a few weak and low-n ATI peaks, the remaining spectrum is very smooth without any of the detailed structure that is visible in the PES for naphthalene even at twice the intensity. Although the differences in the photoabsorption cross sections and the *IE*s of the molecules may play a role, the comparison nevertheless demonstrates that quasi-thermal processes are considerably less important for naphthalene. Also the striking evidence for Freeman resonances indicates that the ionization is more similar to atomic ionization than the ionization of larger molecules is, e.g., anthracene. This is remarkable because the difference between the two molecules is two vs. three aromatic rings.

For both targets an intermediate photoabsorption state exists and takes part in the ionization mechanism. However, the vertical ionization is more pronounced for naphthalene than for anthracene. Moreover, a significant difference appears in the dependence of PES on pulse duration. For naphthalene, variation of the duration

between 150 and 660 fs causes little change in the spectral feature, whereas for anthracene, a change even from 150 to 300 fs clearly suppresses the vertical ionization yield. These observations lead to the conclusion that the IC rate is slower for naphthalene than for anthracene, and that this difference cause the different ionization behavior of these two molecules.

4. Conclusion

We have measured PES on naphthalene excited with a hundred femtosecond, 775 nm pulse and compared to analogous results for larger molecules, primarily anthracene, with the aim to determine the effect of the reduced molecular size on the relative importance of the different ionization mechanisms. The PES of naphthalene are generated by mechanisms that involve Freeman resonances, and the ionization mechanisms closely resemble those that are effective for atoms. From the laser pulse duration dependence of the spectra, the IC rate is found to be smaller for naphthalene than for anthracene, which is one of the main reasons for the different ionization behavior of these two molecules. This emphasizes the importance of the IC rate for determining the ionization mechanism of molecules.

Acknowledgment

This work has been supported by the Swedish Research Council (VR), Stiftelsen för Internationalisering av högre utbildning och forskning (STINT).

References

[1] P. Agostini, F. Fabre, G. Mainfray, G. Petite, N.K. Rahman, Phys. Rev. Lett. 42 (1979) 1127.
[2] R.R. Freeman, P.H. Bucksbaum, H. Milchberg, S. Darack, D. Schumacher, M.E. Geusic, Phys. Rev. Lett. 59 (1987) 1092.
[3] C.P. Schick, P.M. Weber, J. Phys. Chem. A 105 (2001) 3725.
[4] E.E.B. Campbell, K. Hansen, K. Hoffmann, G. Korn, M. Tchaplyguine, M. Wittmann, I.V. Hertel, Phys. Rev. Lett. 84 (2000) 2128.
[5] M. Kjellberg, O. Johansson, F. Jonsson, A.V. Bulgakov, C. Bordas, E.E.B. Campbell, K. Hansen, Phys. Rev. A 81 (2010) 023202.
[6] M. Maier, M.A. Hoffmann, B. von Issendorff, New J. Phys. 5 (2003) 3.
[7] M. Kjellberg, A.V. Bulgakov, M. Goto, O. Johansson, K. Hansen, J. Chem. Phys. 133 (2010) 074308.
[8] M. Goto, K. Hansen, J. Chem. Phys. 135 (2011) 214310.
[9] C. Bordas, F. Paulig, H. Helm, D.L. Huestis, Rev. Sci. Instrum. 67 (1996) 2257.
[10] W. Schmidt, J. Chem. Phys. 66 (1977) 828.
[11] M.J. DeWitt, R.J. Levis, Phys. Rev. Lett. 81 (1998) 5101.
[12] N. Kuthirummal, P.M. Weber, Chem. Phys. Lett. 378 (2003) 647.
[13] N. Kuthirummal, P.M. Weber, J. Mol. Struct. 787 (2006) 163.
[14] N.P. Moore, R.J. Levis, J. Chem. Phys. 112 (2000) 1316.
[15] P. Ludowise, M. Blackwell, Y. Chen, Chem. Phys. Lett. 258 (1996) 530.
[16] K. Hansen, K. Hoffmann, E.E.B. Campbell, J. Chem. Phys. 119 (2003) 2513.